

Analysis of Power to Apparent Power Ratio in EMG signals using Windowing Method for Paralytic Patients

Hemant kr. Gupta

*Department of Electronics & Communication engineering
Arya College of Engineering & I.T. Jaipur*

Prof. Ritu Vijay

*Department of Electronics engineering
Banasthali University Jaipur*

Abstract: Detection of EMG signals with powerful and advance methodologies are becoming a very important requirement in biomedical engineering. The main reason for the interest in EMG signal analysis is in clinical diagnosis and biomedical applications. The field of management and rehabilitation of motor disability is identified as one of the important application areas. The shapes and firing rates of Motor Unit Action Potentials (MUAPs) in EMG signals provide an important source of information for the diagnosis of neuromuscular disorders. In this paper, we introduce an MATLAB based algorithm for processing of sEMG signals of paralytic patients. The power to apparent power ratio has been investigated using Hamming window, Hanning window and Rectangular window. In this paper ten paralytic subjects have contributed by performing different finger movement activities.

Keywords: sEMG, Window, Paralytic, Power, apparent power

I. INTRODUCTION

When a muscle contracts, the neuromuscular activities associated with that muscle results in myoelectric signals being generated which we call as EMG. It is a common practice to measure the skin surface EMG signals in order to identify the intention of an individual [5]. For example if we want to build any prosthetic or orthotic device, we will need to know the intention of the users. One solution is to use EMG signals. There are various factors involved in the development, recording and analysis of myoelectric signals.

Measurement of EMG signal is corrupted by additive noise whose signal to- noise ratio (SNR) varies in an unknown manner [6]. Unlike the classical Neurological EMG, where an artificial muscle response due to external electrical stimulation is analyzed under static conditions, the focus of Kinesiological EMG can be described as the study of the neuromuscular activation of muscles within postural tasks, functional movements, work conditions and treatment/training regimes [7]. The EMG is considered as a reasonable reflection of the muscle activity [8], which indicates the firing rate of motor neurons.

Each individual has his own style of using his muscles for a certain motion and one muscle is associated with more than one motion task [9]. This fuzzy behavior of biological signals such as EMG has been noted many years back [10]. Analysis of EMG data can be done using raw signal (prior to any processing) or using processed signal. The raw data is not very useful for classification purposes. Hence, it is usually processed and used for further analyses.

II. EMG GENERATION AND ACQUISITION

The EMG signal represents the electrical manifestation associated with a muscle contraction. The origin of the signal lays deep in the motor cortex of the human brain, where an electrical impulse is generated. From here, the impulse is transported through neural fibers until it reaches the motor neuron located in the spinal cord. From this point, afferent and efferent fibers drive impulses towards and from the muscle in a complex scheme, to provide a precise control of the force generated by the muscle and leading to the possibility of controlling the position and movement speed of the limb. The single motor neuron and the muscle fibers it innervates is named motor unit and it represents the basic control structure involved in muscle contraction.

The signal collected over a period of time is related to the force developed by the muscle. By studying the correlation between finger pressure and EMG activity of the forearm, patterns in EMG signal could be associated with a certain finger action and hence, those signals could be used in a system like prosthesis or in keyboard

commands for disabled people. The acquisition of EMG signals can be done by EMG sensors, which usually are electrodes of Ag and AgCl placed intramuscular or at the surface of the skin. To provide the reference potential, a patient reference electrode is placed over a zone with little or no muscular activity.

III. DATA COLLECTION

Ten subjects, Eight males and two females, aged between 40 and 65 years were recruited to perform the required fingers movements. The subjects were all paralytic Patients with one side neurological or muscular disorders. All participants provided informed consent prior to participating in the study. Subjects were lying on bed, with their arm supported and fixed at one position to avoid the effect of different limb positions on the generated EMG signals (Scheme, Founger, Stavdahl, Chan, & Englehart, 2010).

The EMG data was collected using one EMG channels (Delsys DE 2.x series EMG sensors) and processed by the Bagnoli Desktop EMG Systems from Delsys Inc. A 2-slot adhesive skin interface was applied on each of the sensors to firmly stick the sensors to the skin. A conductive adhesive reference electrode (Dermatode Reference Electrode) was utilized on the wrist of each subject. The positions of these electrodes are shown in Fig. 1. The EMG signals collected from the electrodes were amplified using a Delsys Bagnoli-8 amplifier to a total gain of 1000. A 12-bit analog-to-digital converter (National Instruments, BNC-2090) was used to sample the signal at 4000 Hz; the signal data were then acquired using Delsys EMGWorks Acquisition software. The EMG signals were then bandpass filtered between 20 and 450 Hz with a notch filter implemented to remove the 50 Hz line interference.



Fig. 1a Position of First Electrode



Fig. 1b Position of Second Electrode

Ten classes of individual and combined fingers movements were implemented including: the flexion of the individual fingers, i.e. Thumb (T), Index (I), Middle (M), Ring (R), Little (L) and the pinching of combined Thumb–Index (T–I), Thumb–Middle (T–M), Thumb–Ring (T–R), Thumb–Little (T–L), and finally the hand close (HC) as shown in Fig. 2.



Fig. 2 Different Movement Classes

IV. SYSTEM MODEL

The AWGN noise has been combined with the clean EMG signal and then noisy signal has been processed using different algorithms which are implemented on MATLAB platform. The AC power flow has three components: real or true power (P) measured in watts (W), apparent power (S) measured in volt-amperes (VA), and reactive power (Q) measured in reactive volt-amperes (VAr). These three types of power are related to each other in a trigonometric form. This is called a power triangle. In this paper the ratio of power to apparent power ratio has been calculated which is an important parameter for medical diagnosis and for human computer interface.

Algorithm 1

- A. Add additive white Gaussian noise AWGN to clean EMG.
- B. Remove DC offset and rectify the signal.

- C. Use 3rd order FIR low pass Butterworth filter.
- D. Calculate power to apparent power ratio.

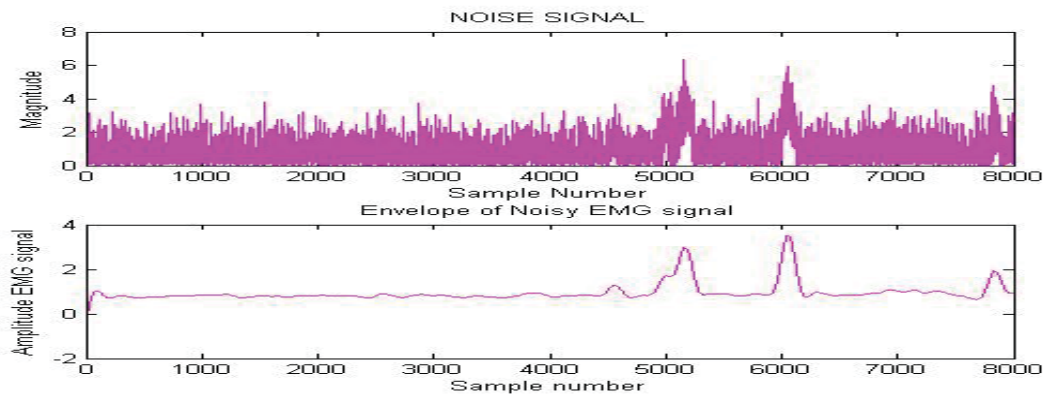


Fig. 3 Representation of noisy signal and its envelope

Flow Chart

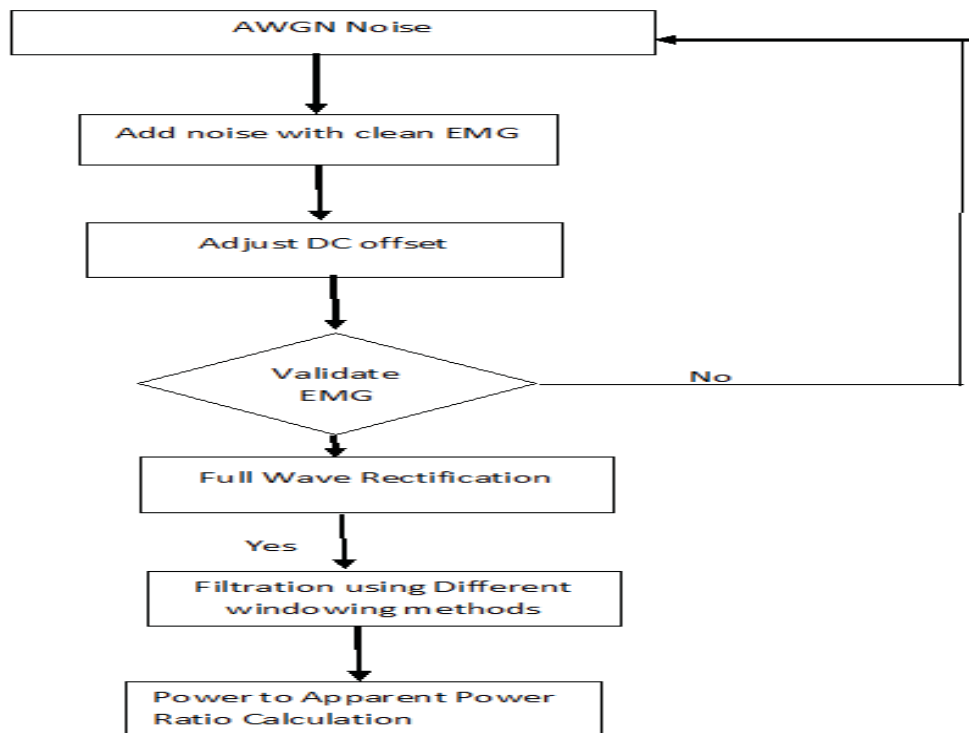


Fig. 4 Flow chart representation of algorithm 1

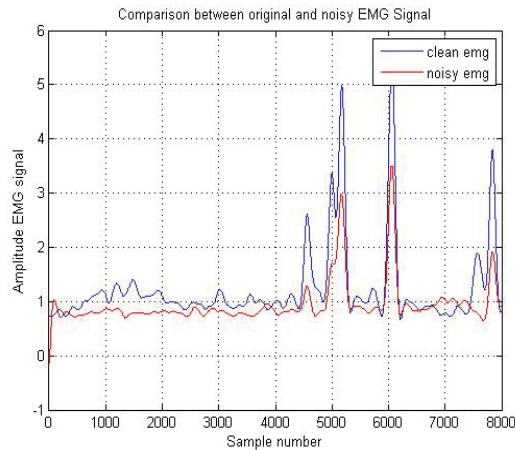


Fig. 5 Amplitude comparison between original and noisy EMG EMG

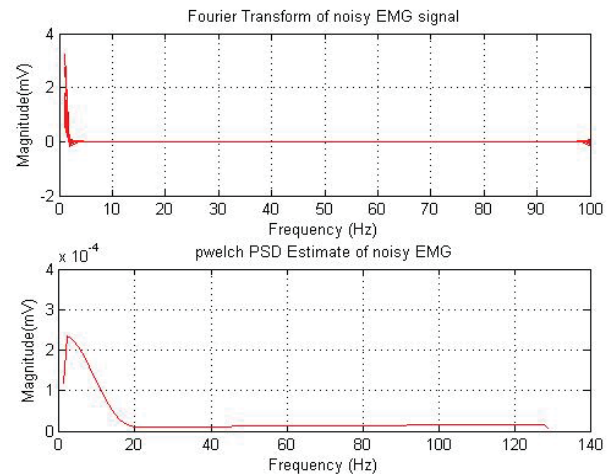


Fig.6 Fourier transform and power spectral density of noisy

Algorithm 2

- A. Apply different windowing methods like hamming window, hanning window and rectangular window on noisy EMG signal for filtering.
- B. Calculate Power to Apparent power ratio for hamming, hanning and rectangular window.
- C. Compare the parameters for different windowing EMG signals and find the best suitable window for processing of EMG signal
- D. Compare the parameters by specific window for various finger movement activities and find the best possible activity for paralytic patients.

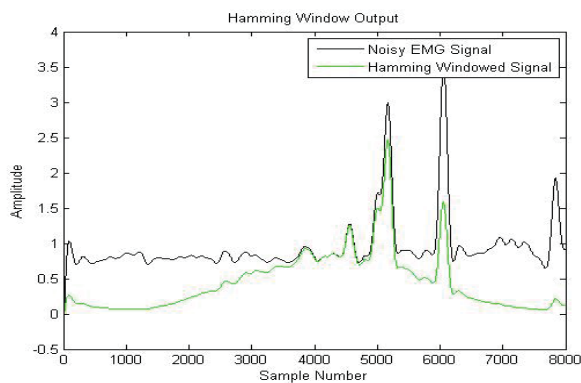


Fig.7 Amplitude comparison between noisy and hamming windowed EMG EMG

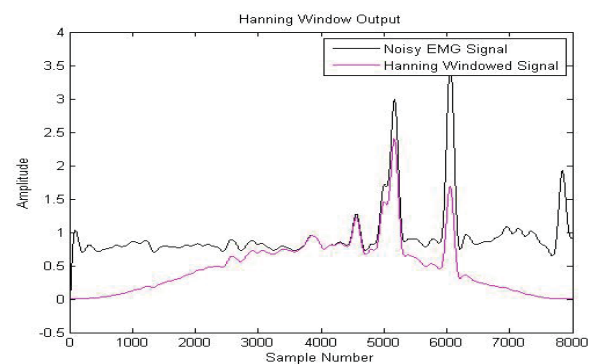


Fig.8 Amplitude comparison between noisy and hamming windowed

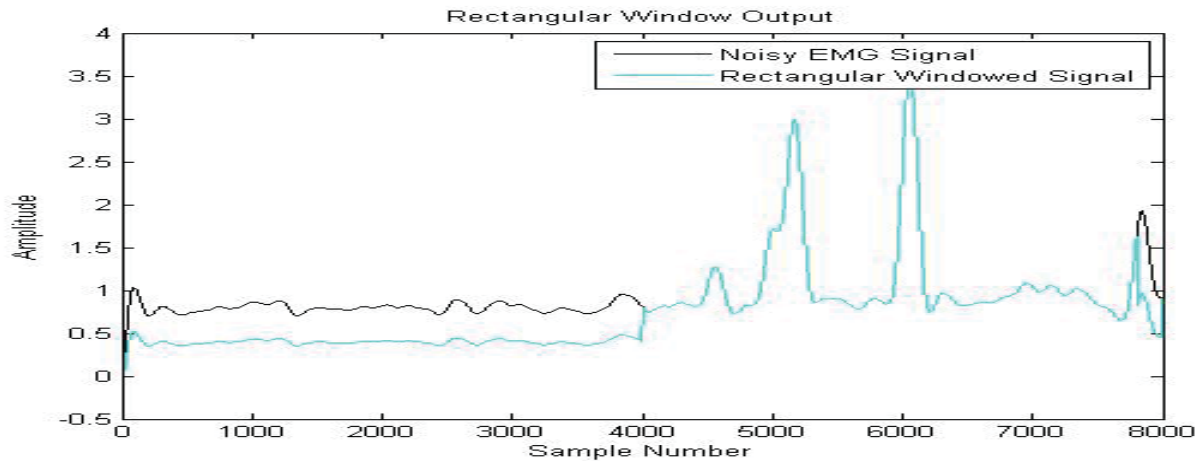


Fig.9 Amplitude comparison between noisy and hamming windowed EMG

Real time results

Table 1 Power to apparent power ratio for Hamming, Hanning and Rectangular Window during performing hand closed activity

| | 1 | 2 | 3 | 4 | 5 | 6 | 7 | 8 | 9 | 10 |
|-------------------------|--------|--------|--------|--------|---------|--------|---------|--------|--------|--------|
| PAPR HAMMING WINDOW | 5.2194 | 4.9634 | 5.0027 | 4.8533 | 5.0717 | 4.8661 | 5.3142 | 4.9988 | 5.2834 | 5.1628 |
| PAPR HANNING WINDOW | 5.4604 | 5.2002 | 5.2506 | 5.0946 | 5.3175 | 5.103 | 5.567 | 5.2228 | 5.5228 | 5.4138 |
| PAPR RECTANGULAR WINDOW | 9.3476 | 9.4209 | 7.4146 | 9.7579 | 10.1318 | 10.375 | 10.0422 | 9.1026 | 9.6117 | 8.529 |

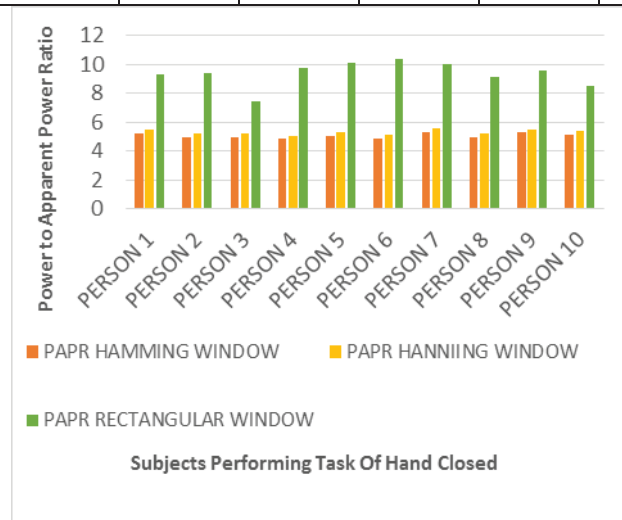


Fig.10 PAPR comparison for different windows during hand closed closed

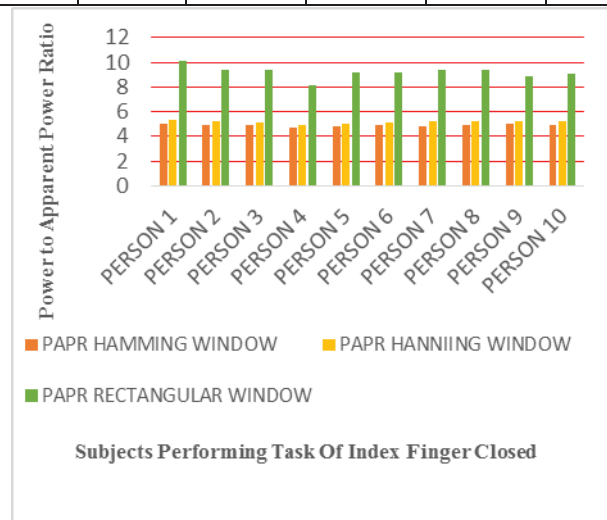


Fig.11 PAPR comparison for different windows during index finger closed

Table 2 Power to apparent power ratio for Hamming, Hanning and Rectangular Window during performing index finger closed activity

| | 1 | 2 | 3 | 4 | 5 | 6 | 7 | 8 | 9 | 10 |
|-------------------------|---------|--------|--------|--------|--------|--------|--------|--------|--------|--------|
| PAPR HAMMING WINDOW | 5.0717 | 4.9634 | 4.8893 | 4.7269 | 4.85 | 4.9202 | 4.7864 | 4.9634 | 5.0043 | 4.9315 |
| PAPR HANNIING WINDOW | 5.3175 | 5.2002 | 5.1422 | 4.9627 | 5.0736 | 5.1627 | 5.2002 | 5.2002 | 5.255 | 5.183 |
| PAPR RECTANGULAR WINDOW | 10.1318 | 9.4209 | 9.3822 | 8.1394 | 9.2194 | 9.2103 | 9.4209 | 9.4209 | 8.8272 | 9.1113 |

Table 3 Power to apparent power ratio for Hamming, Hanning and Rectangular Window during performing little finger closed activity

| | PERS ON 1 | PERS ON 2 | PERSO N 3 | PERS ON 4 | PERSO N 5 | PERSO N 6 | PERS ON 7 | PERS ON 8 | PER SON 9 | PERSO N 10 |
|-------------------------|-----------|-----------|-----------|-----------|-----------|-----------|-----------|-----------|-----------|------------|
| PAPR HAMMING WINDOW | 5.0481 | 5.0027 | 5.4781 | 5.4781 | 5.0707 | 5.0707 | 5.164 | 5.0027 | 5.3237 | 5.1965 |
| PAPR HANNIING WINDOW | 5.2929 | 5.2506 | 5.7187 | 5.7187 | 5.31 | 5.31 | 5.2506 | 5.2506 | 5.5743 | 5.4484 |
| PAPR RECTANGULAR WINDOW | 8.6755 | 7.4146 | 9.1618 | 9.1618 | 8.5216 | 8.5216 | 7.4146 | 7.4146 | 8.9388 | 10.1382 |

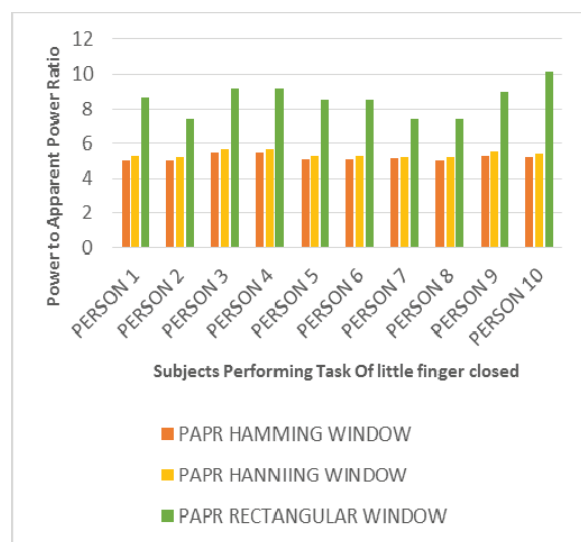


Fig.12 PAPR comparison for different windows during little finger closed

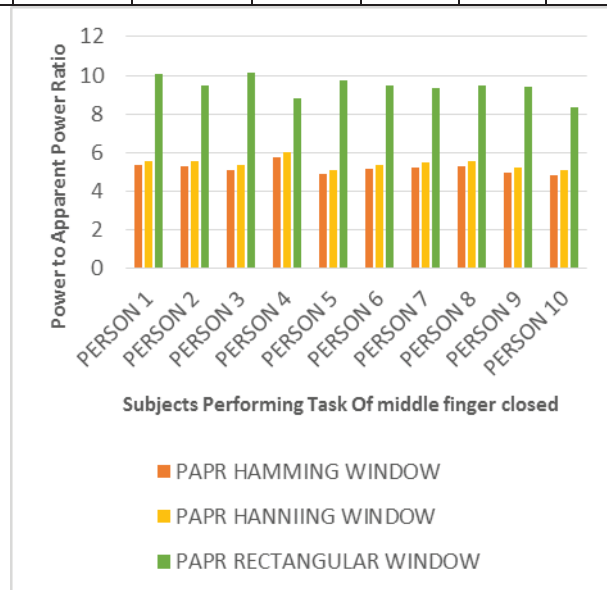


Fig. 13 PAPR comparison for different windows during middle finger closed

Table 4 Power to apparent power ratio for Hamming, Hanning and Rectangular Window during performing middle finger closed activity

| | PERSO N 1 | PERS ON 2 | PERS ON 3 | PERSON 4 | PERS ON 5 | PERSON 6 | PERS ON 7 | PERS ON 8 | PERSON 9 | PERSON 10 |
|-----------------------------------|--------------|--------------|--------------|-------------|--------------|-------------|--------------|--------------|-------------|--------------|
| PAPR HAMMIN G WINDOW | 5.3142 | 5.2944 | 5.0717 | 5.7407 | 4.8533 | 5.1188 | 5.2194 | 5.2944 | 4.9634 | 4.8427 |
| PAPR HANNIIN G WINDOW | 5.567 | 5.5288 | 5.3175 | 5.9903 | 5.0946 | 5.3734 | 5.4604 | 5.5288 | 5.2002 | 5.0944 |
| PAPR RECTAN GULAR WINDOW | 10.0422 | 9.474 | 10.131 8 | 8.81 | 9.7579 | 9.4627 | 9.3476 | 9.4739 | 9.4209 | 8.3125 |

Table 5 Power to apparent power ratio for Hamming, Hanning and Rectangular Window during performing ring finger closed activity

| | PERSO N 1 | PERSO N 2 | PERSO N 3 | PERSO N 4 | PERSON 5 | PERSO N 6 | PERS ON 7 | PERS ON 8 | PERSO N 9 | PERSON 10 |
|---|--------------|--------------|--------------|--------------|-------------|--------------|--------------|--------------|--------------|--------------|
| PAPR HAMM ING WIND OW | 5.1272 | 4.9988 | 4.8662 | 5.2535 | 5.1272 | 5.2729 | 4.9634 | 4.9988 | 5.0027 | 5.3608 |
| PAPR HANNI ING WIND OW | 5.3757 | 5.2228 | 5.103 | 5.4976 | 5.3757 | 5.5259 | 5.2002 | 5.2228 | 5.2506 | 5.6098 |
| PAPR RECTA NGUL AR WIND OW | 10.1525 | 9.1026 | 10.375 | 8.4242 | 10.1525 | 9.8267 | 9.4209 | 9.1026 | 7.4146 | 8.4803 |

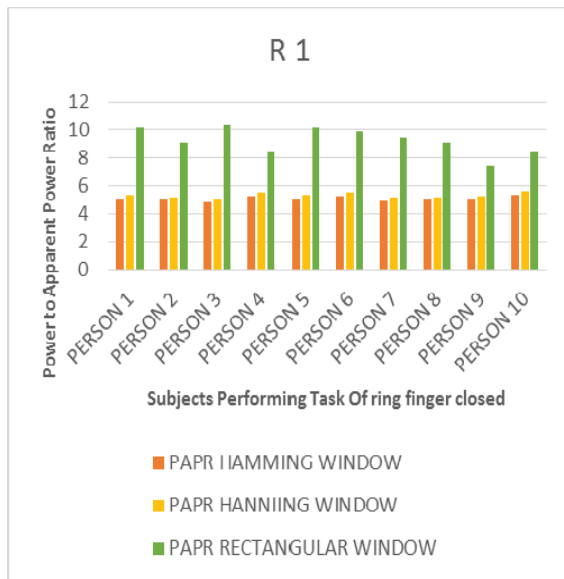


Fig. 14 PAPR comparison for different windows during ring finger closed

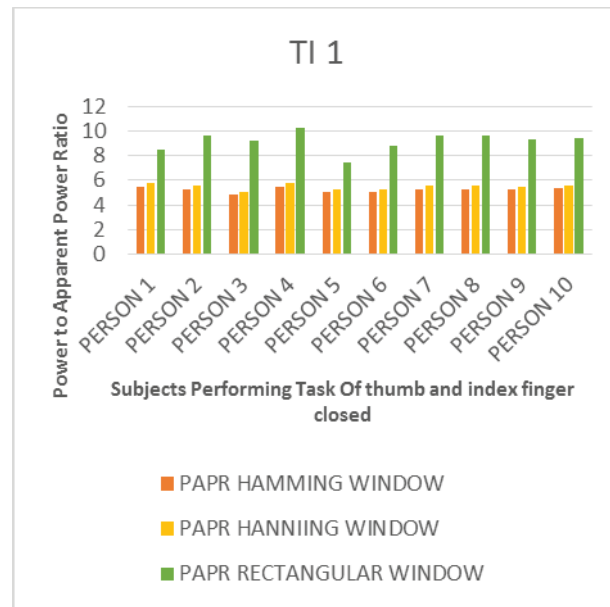


Fig.15 PAPR comparison for different windows during thumb and index closed

Table 6 Power to apparent power ratio for Hamming, Hanning and Rectangular Window during performing thumb and index finger closed activity

| | PERSO N 1 | PERS ON 2 | PERSO N 3 | PERSO N 4 | PERSO N 5 | PERS ON 6 | PERS ON 7 | PERS ON 8 | PERSO N 9 | PERSON 10 |
|---------------------------------------|--------------|--------------|--------------|--------------|--------------|--------------|--------------|--------------|--------------|--------------|
| PAPR HAMMI NG WINDO W | 5.5001 | 5.283 4 | 4.85 | 5.488 | 5.0027 | 5.0043 | 5.2834 | 5.2834 | 5.2194 | 5.3478 |
| PAPR HANNII NG WINDO W | 5.7482 | 5.522 8 | 5.0736 | 5.7311 | 5.2506 | 5.255 | 5.5228 | 5.5228 | 5.4604 | 5.5928 |
| PAPR RECTAN GULAR WINDO W | 8.4364 | 9.611 7 | 9.2194 | 10.2337 | 7.4146 | 8.8272 | 9.6117 | 9.6117 | 9.3476 | 9.4519 |

Table 7 Power to apparent power ratio for Hamming, Hanning and Rectangular Window during performing thumb and little finger closed activity

| | PERSON 1 | PERS ON 2 | PERSON 3 | PERSON 4 | PERSO N 5 | PERS ON 6 | PERS ON 7 | PERSON 8 | PERSO N 9 | PERSO N 10 |
|-------------------------------|-------------|--------------|-------------|-------------|--------------|--------------|--------------|-------------|--------------|---------------|
| PAPR HAMMIN G WINDOW | 5.0481 | 5.1628 | 5.0707 | 5.1769 | 5.2944 | 5.3237 | 5.1628 | 5.3236 | 4.9634 | 5.3062 |
| PAPR HANNIIN G | 5.2929 | 5.4138 | 5.31 | 5.4307 | 5.5288 | 5.5743 | 5.4138 | 5.5742 | 5.2002 | 5.563 |

| WINDOW | | | | | | | | | | |
|-------------------------|--------|-------|--------|--------|-------|--------|-------|--------|--------|-------|
| PAPR RECTANGULAR WINDOW | 8.6755 | 8.529 | 8.5216 | 9.3006 | 9.474 | 8.9387 | 8.529 | 8.9388 | 9.4209 | 9.804 |

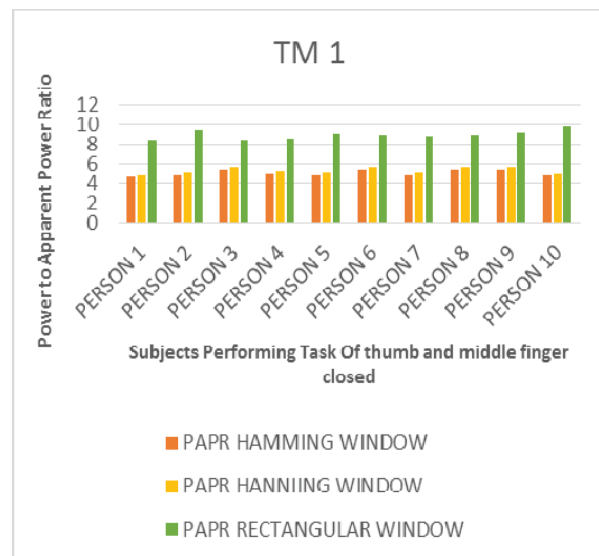
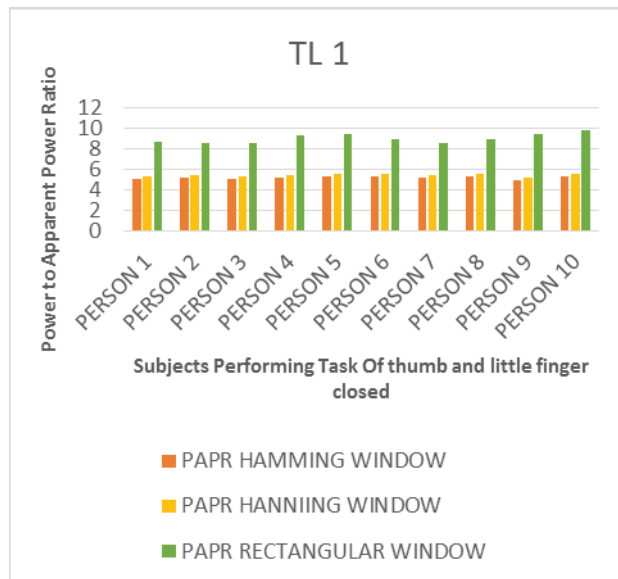


Fig.16 PAPR comparison for different windows during TI finger closed

Fig.17 PAPR comparison for different windows during TM finger closed

Table 8 Power to apparent power ratio for Hamming, Hanning and Rectangular Window during performing thumb and middle finger closed activity

| | PERSO N 1 | PERS ON 2 | PERSO N 3 | PERSON 4 | PERS ON 5 | PERSO N 6 | PERSO N 7 | PERS ON 8 | PERSO N 9 | PERSON 10 |
|---|--------------|--------------|--------------|-------------|--------------|--------------|--------------|--------------|--------------|--------------|
| PAPR HAMMI NG WINDO W | 4.6633 | 4.8893 | 5.5001 | 5.0294 | 4.9988 | 5.3831 | 4.8921 | 5.383 2 | 5.4781 | 4.8533 |
| PAPR HANNII NG WINDO W | 4.8048 | 5.1422 | 5.7482 | 5.2616 | 5.2228 | 5.6316 | 5.1489 | 5.631 6 | 5.7187 | 5.0946 |
| PAPR RECTA NGULA R WINDO W | 8.4391 | 9.3822 | 8.4365 | 8.4901 | 9.1026 | 8.9682 | 8.809 | 8.968 2 | 9.1618 | 9.7579 |

Table 9 Power to apparent power ratio for Hamming, Hanning and Rectangular Window during performing thumb and ring finger closed activity

| | PERSO N 1 | PERSO N 2 | PERSO N 3 | PERS ON 4 | PERSO N 5 | PERS ON 6 | PERS ON 7 | PERS ON 8 | PERSO N 9 | PERSO N 10 |
|---|--------------|--------------|--------------|--------------|--------------|--------------|--------------|--------------|--------------|---------------|
| PAPR HAMM ING WIND OW | 5.0232 | 4.7269 | 5.2676 | 5.1852 | 5.2834 | 4.931 4 | 5.1272 | 4.9315 | 5.1188 | 4.85 |
| PAPR HANNI ING WIND OW | 5.2787 | 4.9627 | 5.5136 | 5.4364 | 5.5228 | 5.183 | 5.3757 | 5.1831 | 5.3734 | 5.0736 |
| PAPR RECTA NGUL AR WIND OW | 8.8333 | 8.1394 | 9.3215 | 7.9938 | 5.6117 | 9.111 3 | 10.152 5 | 9.1113 | 9.4627 | 9.2194 |

Table 10 Power to apparent power ratio for Hamming, Hanning and Rectangular Window during performing thumb closed activity

| | PERS ON 1 | PERS ON 2 | PERSO N 3 | PERS ON 4 | PERSO N 5 | PERS ON 6 | PERSON 7 | PERSO N 8 | PERSO N 9 | PERSON 10 |
|---|--------------|--------------|--------------|--------------|--------------|--------------|-------------|--------------|--------------|--------------|
| PAPR HAM MING WIND OW | 4.8929 | 4.7248 | 5.122 | 4.9977 | 5.1628 | 5.1965 | 5.2194 | 5.1965 | 5.2729 | 5.4781 |
| PAPR HANN ING WIND OW | 5.1268 | 4.9796 | 5.3697 | 5.2292 | 5.4138 | 5.4485 | 5.4604 | 5.4484 | 5.5259 | 5.7187 |
| PAPR RECT ANGU LAR WIND OW | 9.4613 | 9.1113 | 9.7051 | 10.036 4 | 8.529 | 10.138 2 | 9.3476 | 10.1382 | 9.8267 | 9.1618 |

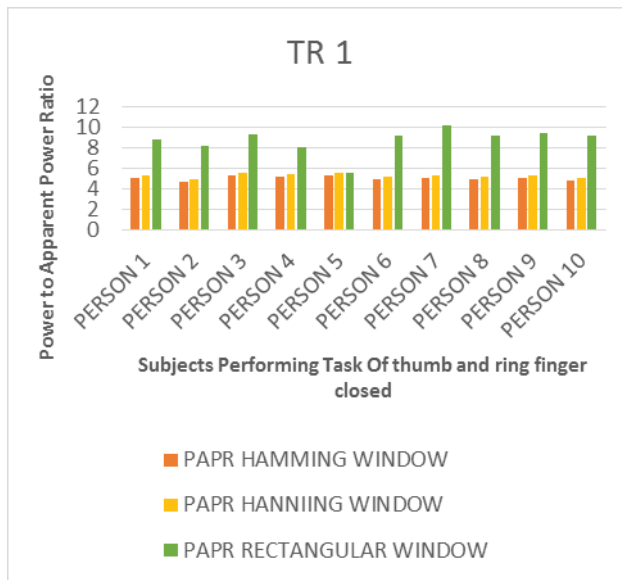


Fig.18 PAPR comparison for different windows during TR finger closed

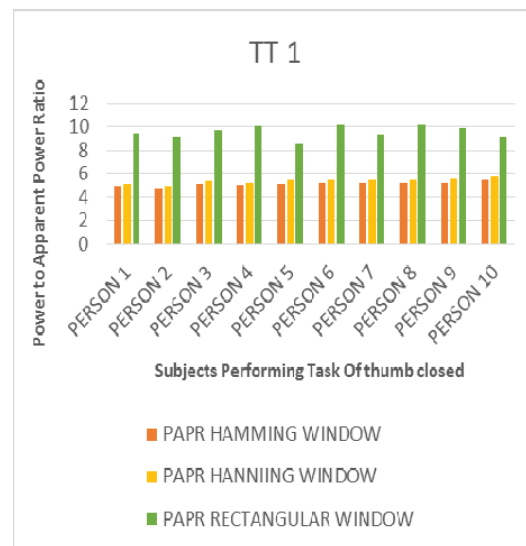


Fig.19 PAPR comparison for different windows during thumb finger closed

V. ANALYSIS

The power to apparent power ratio for three windowing methods has been considered in this paper. It is observed that rectangular window have highest power to apparent power ratio with respect to hamming and hanning window. Hanning window have larger PAPR than hamming window. Rectangular window have 80% more PAPR than hamming and hanning window. Hamming window have 5% less PAPR than hanning window.

The proposed digital processing Technique can be extensively used in bio-medical engineering field. This can also be used in précised equipment manufacturing for low signal analysis.

VI. CONCLUSION

The proposed method is highly effective in analyzing the EMG signals. It is easy to use & apply in real time processing of any random signal obtained from the bio-medical sensors. In this paper, we developed an algorithm on MATLAB for calculating power to apparent power ratio using Hamming, Hanning and Rectangular window for various activities performed by paralysis patients. From result studies, we observe that the proposed method is highly effective & efficient.

REFERENCES

- [1] L. Echternach. Introduction to Electromyography and Nerve Conduction Testing. Slack Inc., 2nd edition, 2003.
- [2] D. Gordon and E. Robertson. Electromyography: Recording. Univerisity of Ottawa, Canada, http://www.health.uottawa.ca/biomech/courses/apa4311/emg_c.pdf accessed 31st July 2005.
- [3] Jang-Zern Tsai. Chapter 7: Nervous system. In J G Webster, editor, Bioinstrumentation. Wiley International, 2004.
- [4] A. Hiraiwa, K. Shimohara, and Y. Tokunaga, "EMG pattern analysis and classification by neural network," in Systems, Man and Cybernetics, 1989. Conference Proceedings. IEEE International Conference on, 1989, pp. 1113-1115 vol.3.
- [5] G. R. Naik, D. K. Kumar, V. P. Singh, and M. Palaniswami, "Hand gestures for HCI using ICA of EMG," in Proceedings of the HCSNet workshop on Use of vision in human-computer interaction-Volume 56, 2006, pp. 67-72.
- [6] K. Englehart, B. Hudgins, M. Stevenson, and P. A. Parker, "A dynamic feed forward neural network for subset classification of myoelectric signal patterns," in Engineering in Medicine and Biology Society, 1995., IEEE 17th Annual Conference, 2002, vol. 1, pp. 819- 820.
- [7] M. F. Naik, P. A. Parker, and R. N. Scott, "The application of neural networks to myoelectric signal analysis: a preliminary study," Biomedical Engineering, IEEE Transactions on, vol. 37, no. 3, pp. 221-230, 2002.
- [8] C. J. De Luca. Surface Electromyography: Detection and Record-ing. Delsys Inc. E-book: <http://www.delsys.com/library/papers/SEMIntro.pdf>, 2002.
- [9] Scheme, E., Founger, A., Stavadahl, O., Chan, A. D. C., & Englehart, K. (2010). Examining the adverse effect of limb position on pattern recognition based myoelectric control. In Proceedings of the 32nd annual international conference of the IEEE EMBS (pp. 6337-6340).
- [10] M. B. I. Reaz, M. S. Hussain, and F. Mohd-Yasin, "Techniques of EMG signal analysis: detection, processing, classification and applications," Biological procedures online, vol. 8, no. 1, pp. 11-35, 2006.